

Performance of TOA and FOA-based Localization for Cospas-Sarsat Search and Rescue Signals

Victor Bissoli Nicolau^{1,2}, Martial Coulon¹, Yoan Grégoire³, Thibaud Calmettes⁴ and Jean-Yves Tourneret¹

¹University of Toulouse, INP-ENSEEIH/IRIT, 2 rue Charles Camichel, 31071 Toulouse Cedex 7, France

²TéSA, 14-16 Port Saint-Etienne, 31000 Toulouse, France ³CNES, 18 Av. Edouard Belin, 31401 Toulouse, France

⁴Thales Alenia Space, 26 Av. Jean-François Champollion, 31037 Toulouse Cedex 1, France

{victor.bissolinicolau, martial.coulon, jean-yves.tourneret}@enseeih.fr

yoan.gregoire@cnes.fr, thibaud.calmettes@thalesaleniaspace.com

Abstract—This work studies the performance of position estimation for distress beacons using time of arrival and frequency of arrival measurements. The analysis is conducted for emergency signals modeled as pulses with sigmoidal transitions. This model has shown interesting properties for Cospas-Sarsat search and rescue signals. The modified Cramér-Rao bounds of the symbol width, time of arrival, frequency of arrival, and position of this model are presented. Simulations conducted with realistic signals indicate good agreement between these bounds and the mean square errors of the estimated parameters.

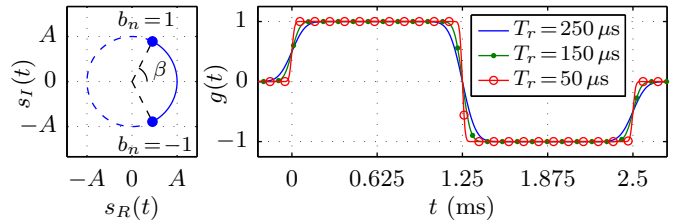
I. INTRODUCTION

The Cospas-Sarsat search and rescue (SAR) system is designed to locate emergency beacons activated by aircrafts, ships and hikers in distress. Localization is performed using low-altitude satellites, through Doppler processing. However, due to the orbit patterns, there can be delays between beacon activation and position determination [1]. To provide faster alerting, SAR instruments are recently being installed on medium earth orbit satellites of the next-generation MEOSAR system. In this scenario, with several satellites in view of the beacon, times of arrival (TOA) are also considered to complement the frequencies of arrival (FOA) already employed [2]. However, the emergency signals that are currently used were not designed to allow good TOA measurement properties.

In this work, we address the localization performance of Cospas-Sarsat beacons. We start from the results of a previous work [3] where we proposed a sigmoidal function to model the signal transitions, and where we derived the modified Cramér-Rao bounds (MCRBs) [4] for the symbol width and the TOA. In this article, we derive the MCRBs for the FOA and the beacon position. The obtained bounds are useful to assess the performance of the system, and to define the weighting matrix of the contributions from TOA and FOA measurements, which is an important step for position estimation. We also analyze the impact of the constellation geometry on the position estimation using the classical geometric dilution of precision (GDOP) [5], and we define an equivalent new figure of merit that takes into account the movement of the satellites.

This paper is organized as follows. Section II presents the signal model with sigmoidal transitions. Section III derives the MCRBs for unbiased estimators of the signal parameters already mentioned, and presents estimation methods. Section IV derives the MCRBs for position estimation, and recalls the classical least squares (LS) method. Simulation results are given in Section V and conclusions are reported in Section VI.

The authors wish to thank the French government space agency (CNES) and Thales Alenia Space for technical advice and funding.



(a) Signal space. (b) Manchester pulse $g(t)$ for different rise times T_r .
Fig. 1. Illustration of (a) signal space of $s(t)$ and (b) Manchester pulse $g(t)$.

II. SIGNAL MODEL

The emergency beacon generates phase-modulated waveforms, using Manchester data encoding. Following the system specifications [6], the received signal can be modeled as

$$r(t) = s(t) + w(t) \quad (1)$$

with

$$s(t) = A \exp \left[j2\pi\nu t + j\beta \sum_{n=0}^{N-1} b_n g(t - nT - \tau) + j\phi_0 \right] \quad (2)$$

where $w(t)$ is a complex white Gaussian noise with two-sided power spectral density of $2N_0$, A is the amplitude, ν is the Doppler shift, β is the modulation index, N is the number of symbols, $\mathbf{b} = \{b_n\}$ is a zero-mean independent and identically distributed (iid) sequence of random variables associated with the information bits, T is the symbol width, τ is the transmission delay and ϕ_0 is the initial phase. Fig. 1(a) shows the signal space, where $s_R(t)$ and $s_I(t)$ are the real and imaginary parts of $s(t)$. Following the system specifications [6] for the signal rise time T_r , in our previous work [3] we represented the pulse $g(t)$ as

$$g(t) = \frac{1}{2} \operatorname{erf}(\alpha t) - \operatorname{erf}[\alpha(t - T/2)] + \frac{1}{2} \operatorname{erf}[\alpha(t - T)] \quad (3)$$

where the choice of the error function as a sigmoidal function was important to evaluate the MCRBs of interest. This is due to its derivative being a Gaussian pulse, which has a simple Fourier transform. The parameter α in (3) can be used to adjust the rise time T_r with [3]

$$\alpha = \frac{2 \operatorname{erf}^{-1}(0.9)}{T_r} \approx \frac{2.3262}{T_r} \quad (4)$$

where $\operatorname{erf}^{-1}(\cdot)$ is the inverse error function. Fig. 1(b) shows the shape of $g(t)$ for the minimum ($T_r = 50 \mu\text{s}$), nominal ($T_r = 150 \mu\text{s}$) and maximum ($T_r = 250 \mu\text{s}$) values allowed for T_r .

III. TOA AND FOA ESTIMATION

In the following, we analyze the performance of TOA and FOA estimation for the SAR signal defined in (2). Section III-A derives the MCRBs of interest, where we consider that receivers share burst data only, i.e., TOA and FOA [1]. Section III-B recalls a classical method to estimate ν whereas Section III-C shows a resampling method to jointly estimate τ and T .

A. MCRBs for the joint estimation of TOA and FOA

Generally, the MCRB is a less reliable bound than the standard Cramér-Rao bound (CRB), but it is much easier to evaluate. While deriving the joint MCRBs for unbiased estimators of τ and ν , we also estimate the symbol width, as this parameter is related to the TOA estimation and varies in the range allowed for the bit rate, $R_s = 1/T = 400 \text{ bps} \pm 1\%$ [6]. Denoting $\boldsymbol{\lambda} = (T, \tau, \nu)^T$ as the unknown parameter vector, the covariance matrix of an unbiased estimator of $\boldsymbol{\lambda}$, denoted $\mathbf{C}_{\hat{\boldsymbol{\lambda}}}$ (where $\hat{\boldsymbol{\lambda}} = (\hat{T}, \hat{\tau}, \hat{\nu})^T$), satisfies the inequality [7]

$$\mathbf{C}_{\hat{\boldsymbol{\lambda}}} - \mathbf{I}_M^{-1}(\boldsymbol{\lambda}) \succeq \mathbf{0} \quad (5)$$

where $\succeq \mathbf{0}$ indicates that the matrix is positive semi-definite and $\mathbf{I}_M(\boldsymbol{\lambda})$ is the 3×3 modified Fisher information matrix (MFIM), whose elements are defined as

$$[\mathbf{I}_M(\boldsymbol{\lambda})]_{ij} = \mathbb{E}_{\mathbf{r}, \mathbf{u}} \left[\frac{\partial \ln p(\mathbf{r}|\mathbf{u}, \boldsymbol{\lambda})}{\partial \lambda_i} \frac{\partial \ln p(\mathbf{r}|\mathbf{u}, \boldsymbol{\lambda})}{\partial \lambda_j} \right]. \quad (6)$$

Note that (6) is easier to evaluate than the classical FIM that contains $p(\mathbf{r}|\boldsymbol{\lambda})$ instead of $p(\mathbf{r}|\mathbf{u}, \boldsymbol{\lambda})$. The vector $\mathbf{r} = (r_1, r_2, \dots, r_\kappa)^T$ is the vector of coefficients obtained from an orthonormal expansion of $r(t)$ using κ orthonormal functions, $\mathbf{u} = (A, \mathbf{b}, \phi_0)^T$ is the nuisance parameter vector and $p(\mathbf{r}|\mathbf{u}, \boldsymbol{\lambda})$ is the probability density function of the observation vector. It is usually more convenient to use a formalism based on continuous waveforms. Indeed, as explained in [8, p. 292], in the limit, as $\kappa \rightarrow \infty$, $p(\mathbf{r}|\mathbf{u}, \boldsymbol{\lambda})$ can be replaced by

$$p(\mathbf{r}|\mathbf{u}, \boldsymbol{\lambda}) \propto \exp \left[-\frac{1}{2N_0} \int_{T_0} |r(t) - s(t)|^2 dt \right] \quad (7)$$

where T_0 is the signal length. Replacing (7) in (6) and following the derivations of [4], the MFIM elements can be written

$$[\mathbf{I}_M(\boldsymbol{\lambda})]_{ij} = \frac{1}{N_0} \mathbb{E}_{\mathbf{u}} \left[\int_{T_0} I_t(\lambda_i, \lambda_j) dt \right] \quad (8)$$

where

$$I_t(\lambda_i, \lambda_j) = \frac{\partial s_R(t)}{\partial \lambda_i} \frac{\partial s_R(t)}{\partial \lambda_j} + \frac{\partial s_I(t)}{\partial \lambda_i} \frac{\partial s_I(t)}{\partial \lambda_j}. \quad (9)$$

The upper left 2×2 block matrix in (8) is related to the estimation of the symbol width and TOA. This matrix was derived in a previous work [3] and will be used in the following. The next part of this section computes $[\mathbf{I}_M(\boldsymbol{\lambda})]_{33}$, which is related to the FOA estimation. Using the notation $\phi_\nu(t) = 2\pi\nu t$, the integrand $I_t(\nu, \nu)$ in (8) can be written

$$I_t(\nu, \nu) = A^2 \left| \frac{\partial \phi_\nu(t)}{\partial \nu} \right|^2 \quad (10)$$

hence

$$[\mathbf{I}_M(\boldsymbol{\lambda})]_{33} = 4\pi^2 \frac{A^2}{N_0} \int_{t_0}^{t_0+T_0} t^2 dt \quad (11)$$

$$= 4\pi^2 \frac{A^2}{N_0} \left(t_0^2 T_0 + t_0 T_0^2 + \frac{T_0^3}{3} \right). \quad (12)$$

The remaining elements of the MFIM are obtained in a similar fashion and can be shown to be zero, i.e., the estimation of (T, τ) is decoupled from the estimation of ν . As the MCRB is a lower bound, we are interested in its maximum value with respect to the integration start time t_0 , that is obtained with $t_0 = -T_0/2$ in (12) [9]. Using (12) and our previous results in [3], the MFIM of $\boldsymbol{\lambda}$ for $t_0 = -T_0/2$ can be written

$$\mathbf{I}_M(\boldsymbol{\lambda}) = \frac{C}{N_0} \begin{bmatrix} \alpha\beta^2 \sqrt{\frac{2}{\pi}} N^3 & 3\alpha\beta^2 \sqrt{\frac{2}{\pi}} \frac{N^2}{2} & 0 \\ 3\alpha\beta^2 \sqrt{\frac{2}{\pi}} \frac{N^2}{2} & 3\alpha\beta^2 \sqrt{\frac{2}{\pi}} N & 0 \\ 0 & 0 & \pi^2 \frac{T_0^3}{3} \end{bmatrix} \quad (13)$$

for $B \geq \alpha\sqrt{2}$, where B is the signal bandwidth and $C = A^2$. The diagonal elements of $\mathbf{I}_M^{-1}(\boldsymbol{\lambda})$ give the MCRBs of interest. Finally, using block-matrix inversion, we obtain

$$\text{MCRB}_J(\tau) = \frac{4}{3} \sqrt{\frac{\pi}{2}} \frac{1}{\alpha\beta^2 \frac{C}{N_0} N}, \quad \text{MCRB}_J(\nu) = \frac{1}{\pi^2 \frac{T_0^3}{3} \frac{C}{N_0}} \quad (14)$$

where the index J indicates joint estimation. Both bounds are inversely proportional to C/N_0 . The TOA estimation is more accurate for shorter rise times, i.e., for larger values of α . This is expected, since fast-rising pulses are easier to detect than slow-rising ones. This bound is also inversely proportional to N , while the bound for FOA estimation is inversely proportional to T_0^3 . These results show that jointly estimating ν with (T, τ) does not affect the parameters estimation performance when compared to the estimation of (T, τ) only. The impact of ν on the position estimation is addressed in Section IV.

B. FFT method for FOA estimation

In order to estimate the FOA, we use an FFT method for the unmodulated carrier at the beginning of the SAR signal. A zero-padding factor of 3 ensures a smooth spectrum estimate and a second order polynomial is fitted around the maximum value to estimate $\hat{\nu}$. We also obtain an estimate of ϕ_0 by taking the phase of the FFT sample corresponding to the maximum of the spectrum [9], which will be useful in Section III-C.

C. Resampling method for TOA and symbol width estimation

The estimation of τ and T is carried out with the so-called resampling method, inspired by the works conducted in [10]. We exploit the cyclic correlation of the signal and the symmetry of the Manchester pulse. First, the initial rotation of the constellation is canceled using the previously obtained $\hat{\phi}_0$. Then, the resulting phase of the received signal is filtered using a matched filter, leading to a sum of triangular functions, which are concave or convex depending on the information bits. The absolute value of the resulting signal is then resampled for different T and τ within a pre-specified grid, whose resolution is chosen sufficiently fine to ensure good estimation (see figure 2). Finally, the values of T and τ maximizing the sum of the resampled signal are used as \hat{T} and $\hat{\tau}$.

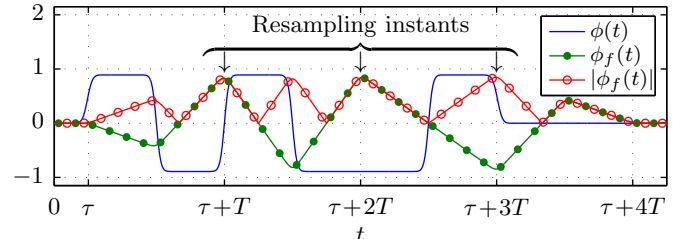


Fig. 2. Matched filtering and resampling of $\phi(t)$ for $\mathbf{b} = (1, 1, -1)$.

IV. POSITION ESTIMATION

This section considers the position estimation of a static beacon, as it is generally the case in emergency situations. We also consider that the downlink is known, i.e., that TOAs and FOAs are acquired at the satellite level. Section IV-A derives the MCRB for unbiased estimators of position using (14) and Section IV-B presents an LS method for position estimation. The TOA and the FOA of the i -th received signal can be written

$$\tau_i = \tau_0 + \frac{\rho_i}{c} + \epsilon_i, \quad \nu_i = \delta_f + f_0 \frac{v_i}{c} + \epsilon_{\nu_i} \quad (15)$$

for $i = 1, \dots, M$, where M is the number of satellites, τ_0 is the transmission time, δ_f is the beacon oscillator deviation, c is the speed of light, ϵ_i and ϵ_{ν_i} are the TOA and the FOA measurement errors, $\rho_i = \|\mathbf{p}_i - \mathbf{p}\|$ and v_i are the distance and the velocity between the beacon and the i -th satellite

$$\mathbf{v}_i = -\mathbf{v}_i^T \mathbf{u}_i(\mathbf{p}), \quad \mathbf{u}_i(\mathbf{p}) = \frac{\mathbf{p}_i - \mathbf{p}}{\rho_i} \quad (16)$$

where \mathbf{v}_i is the velocity vector for the i -th satellite. We can remove the unknowns τ_0 and δ_f from (15) by calculating time differences of arrival (TDOA) and frequency differences of arrival (FDOA). Taking τ_1 and ν_1 as references, we obtain

$$\tau_{1i} = \frac{\rho_{1i}}{c} + \epsilon_{1i}, \quad \nu_{1i} = f_0 \frac{v_{1i}}{c} + \epsilon_{\nu_{1i}}, \quad i = 2, \dots, M \quad (17)$$

with $\tau_{1i} = \tau_1 - \tau_i$, $\rho_{1i} = \rho_1 - \rho_i$, $\epsilon_{1i} = \epsilon_1 - \epsilon_i$, $\nu_{1i} = \nu_1 - \nu_i$, $v_{1i} = v_1 - v_i$, and $\epsilon_{\nu_{1i}} = \epsilon_{\nu_1} - \epsilon_{\nu_i}$. Defining the TDOA and FDOA vector $\boldsymbol{\theta} = (\tau_{12}, \tau_{13}, \dots, \tau_{1M}, \nu_{12}, \nu_{13}, \dots, \nu_{1M})^T$, we define the covariance matrix \mathbf{C}_θ associated with the errors in (17) as

$$\mathbf{C}_\theta = \begin{bmatrix} \mathbf{A} \mathbf{C}_\tau \mathbf{A}^T & \mathbf{0} \\ \mathbf{0} & \mathbf{A} \mathbf{C}_\nu \mathbf{A}^T \end{bmatrix} \quad (18)$$

where $\mathbf{A} = [\mathbf{1}_{M-1}, -\mathbf{I}_{M-1}]$ is composed of an $(M-1) \times 1$ vector of ones and the $(M-1) \times (M-1)$ identity matrix, \mathbf{C}_τ and \mathbf{C}_ν are diagonal covariance matrices for the errors in (15).

A. MCRB for position estimation

The bound for an unbiased estimator of the beacon position $\mathbf{p} = (x, y, z)^T$ can be obtained from (18) using the rule regarding transformation of parameters [7, p. 45]. Thus,

$$\text{MCRB}(p_i) = [(\mathbf{G}^T \mathbf{C}_\theta^{-1} \mathbf{G})^{-1}]_{ii}, \quad i = 1, \dots, 3 \quad (19)$$

with $\mathbf{G} = [\mathbf{G}_\tau^T, \mathbf{G}_\nu^T]^T$ and the lines of \mathbf{G}_τ and \mathbf{G}_ν given by

$$\frac{\partial \tau_{1i}}{\partial \mathbf{p}} = \frac{1}{c} [\mathbf{u}_i(\mathbf{p}) - \mathbf{u}_1(\mathbf{p})]^T, \quad \frac{\partial \nu_{1i}}{\partial \mathbf{p}} = \frac{1}{c} [\chi_i(\mathbf{p}) - \chi_1(\mathbf{p})]^T \quad (20)$$

with

$$\chi_i(\mathbf{p}) = f_0 \frac{\mathbf{u}_i(\mathbf{p}) \mathbf{u}_i^T(\mathbf{p}) - \mathbf{I}}{\rho_i} \mathbf{v}_i, \quad i = 2, \dots, M. \quad (21)$$

The position estimation depends on the constellation geometry (via \mathbf{G}) and on the measurement accuracy (via \mathbf{C}_θ and the bounds (14) that define \mathbf{C}_τ and \mathbf{C}_ν), as expected.

B. Position estimation using the LS method

To estimate the position, we linearize (17) around an estimate $\mathbf{p}_k = (x_k, y_k, z_k)^T$. For $M \geq 3$, the LS estimator and the variances of its components are

$$\hat{\mathbf{p}} = \mathbf{p}_k + (\mathbf{G}_k^T \mathbf{C}_\theta^{-1} \mathbf{G}_k)^{-1} \mathbf{G}_k^T \mathbf{C}_\theta^{-1} (\boldsymbol{\theta} - \boldsymbol{\theta}_k) \quad (22)$$

$$\text{var}(\hat{p}_i) = [(\mathbf{G}_k^T \mathbf{C}_\theta^{-1} \mathbf{G}_k)^{-1}]_{ii}, \quad i = 1, \dots, 3 \quad (23)$$

with $\boldsymbol{\theta}_k = (\tau_{2k}, \tau_{3k}, \dots, \tau_{Mk}, \nu_{2k}, \nu_{3k}, \dots, \nu_{Mk})^T$, $\tau_{ik} = \frac{\rho_{1i}}{c} |_{\mathbf{p}=\mathbf{p}_k}$, $\nu_{ik} = f_0 \frac{v_{1i}}{c} |_{\mathbf{p}=\mathbf{p}_k}$ and $\mathbf{G}_k = \mathbf{G} |_{\mathbf{p}=\mathbf{p}_k}$. Note that the variance (23) equals the bound (19) when \mathbf{p}_k is the true beacon position.

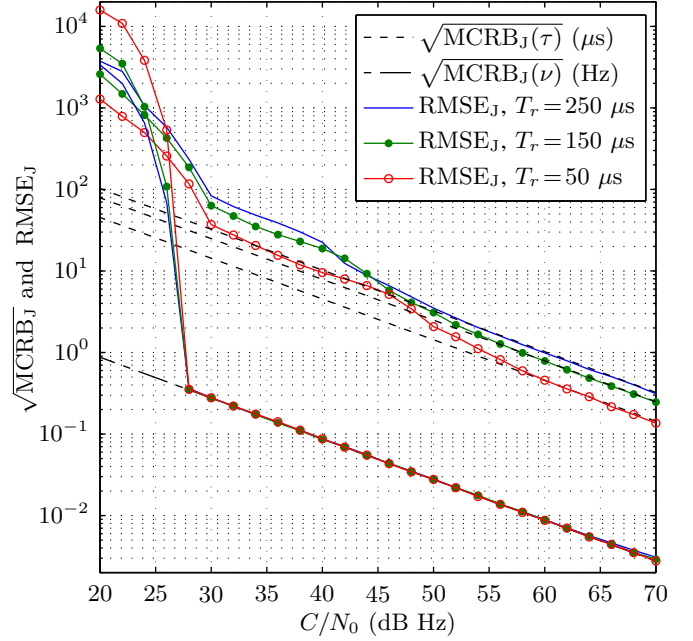


Fig. 3. Estimation of TOA and FOA for different rise times T_r .

V. SIMULATION RESULTS

This section compares the derived MCRBs of TOA, FOA and beacon position with the root mean square errors (RMSEs) of the proposed estimators. Table I provides the simulation parameters, following the distress beacon specifications [6].

Fig. 3 shows the effect of the rise time of the Manchester pulse on TOA and FOA estimators for the minimum, nominal and maximum values allowed for T_r . It is interesting to note that the RMSEs of the conventional estimators (that have not been designed specifically for signal containing smooth sigmoidal transitions) proposed in sections III-B and III-C have good performance for SAR signals and attain the bounds (14) for larger C/N_0 . Therefore, in this C/N_0 region, the derived MCRBs equal the standard CRBs for the considered signal model. For lower C/N_0 , there is a threshold effect, as it is typically exhibited by nonlinear estimators [7]. Moreover, as predicted by (14), the FOA estimator is not affected by T_r .

In order to analyze the position estimation performance, we use the classical GDOP which is an indicator of the satellite-receiver geometry defined as

$$\text{GDOP} = \sqrt{\text{Tr}[(\mathbf{H}^T \mathbf{H})^{-1}]} \quad (24)$$

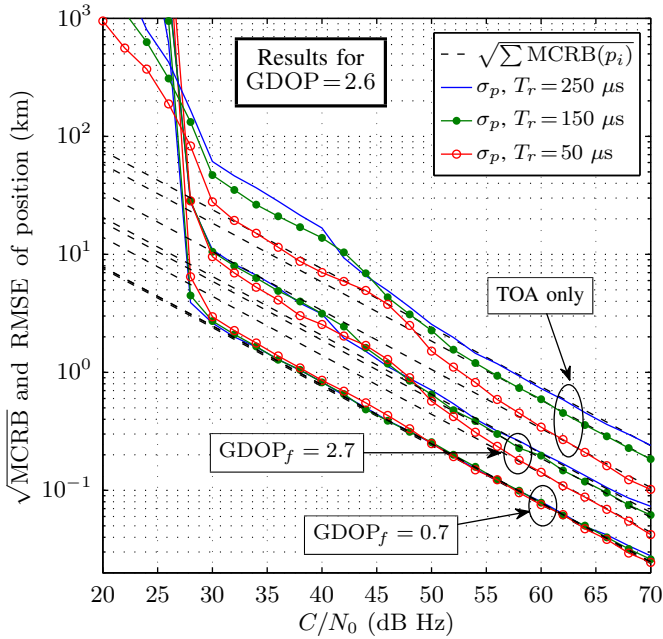
with

$$\mathbf{H} = \begin{bmatrix} \mathbf{u}_1(\mathbf{p}) & \mathbf{u}_2(\mathbf{p}) & \dots & \mathbf{u}_M(\mathbf{p}) \\ 1 & 1 & \dots & 1 \end{bmatrix}^T \quad (25)$$

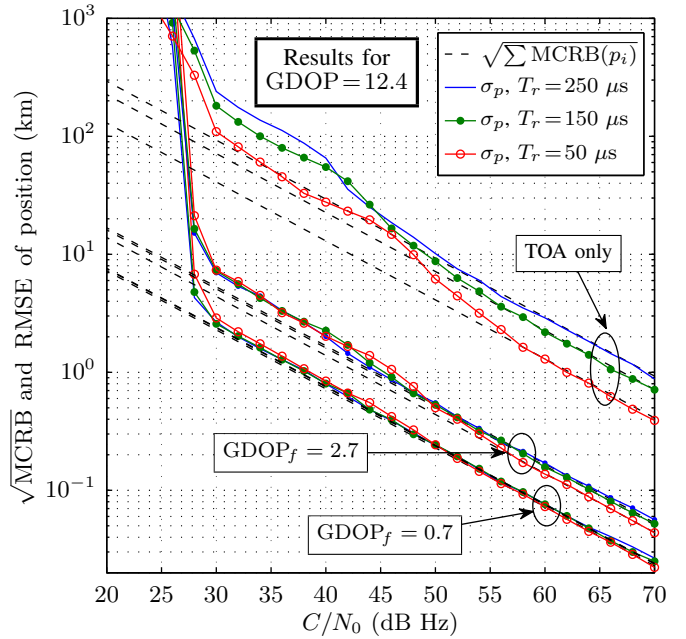
where $\text{Tr}(\cdot)$ denotes the trace operator and the matrix \mathbf{H}

TABLE I. SIMULATION PARAMETERS.

Parameter	Symbol	Value	Unit
Number of symbols	N	144	symbols
Modulation index	β	1.1	radians
Symbol rate	R_s	404	symbols/s
Bandwidth	B	$\alpha\sqrt{2}$	Hz
Carrier frequency	f_0	406	MHz
Unmodulated carrier duration	T_c	160	ms
Number of messages	N_m	5000	messages
Number of satellites	M	4	satellites



(a) Good geometries (GDOP = 2.6).



(b) Poor geometries (GDOP = 12.4).

Fig. 4. Estimation of beacon position for (a) good geometries and (b) poor geometries considering different values of the rise times T_r and GDOP_f .

contains the units vectors pointing from the beacon to the i -th satellite. However, the GDOP does not take into account the movement of the satellites, which also affects the performance of position estimation. Thus we define an equivalent figure of merit, called GDOP_f , that is obtained after replacing the vectors $\mathbf{u}_i(\mathbf{p})$ by $\chi_i(\mathbf{p})$ in (25). We also propose to compare the sum of the variances associated with the x , y and z components (as in [11]) defined as

$$\sigma_p^2 = \mathbb{E}[(\mathbf{p} - \hat{\mathbf{p}})^T (\mathbf{p} - \hat{\mathbf{p}})] = \text{var}(\hat{x}) + \text{var}(\hat{y}) + \text{var}(\hat{z}). \quad (26)$$

The LS method iterates (22) from an initial estimate of the position, obtained from the mean position vector of the satellites. We assume that the weighting matrix \mathbf{C}_θ^{-1} in (22) and (23) is known, since it is built with (18) and the bounds (14).

Fig. 4 compares the MCRBs for position estimation in (19) with the RMSEs of the LS estimator, for good geometries (GDOP = 2.6) and poor geometries (GDOP = 12.4), showing a good agreement for higher values of C/N_0 . Fig. 4 also presents the results for the case where only TOA measurements are available and we notice the advantages of using joint TOAs and FOAs in position calculation. Finally, Fig. 4 shows the impact of GDOP_f , where we notice that, for a same GDOP, the localization accuracy can be favored ($\text{GDOP}_f = 0.7$) or compromised ($\text{GDOP}_f = 2.7$) by the movement of the satellites. That is, the impact of GDOP_f is significant for position estimation and should be considered additionally to the classical GDOP.

VI. CONCLUSION

In this article, we studied the localization performance of distress beacons considering TOA and FOA measurements for emergency signals from the Cospas-Sarsat system. Based on a sigmoidal model of the modulation, the modified Cramér-Rao bounds for the whole localization process have been established. It was verified through simulations that these bounds, computed for the sigmoidal search and rescue signal

model, are very tight for classical estimators. The obtained bounds are useful to assess the performance of the system, since they explicitly depend on the parameters of the signal and on the constellation characteristics. These expressions can also be used to optimize the next-generation MEOSAR system, and to define the weighting matrix of the contributions from TOA and FOA measurements. Future works should consider exploiting measures over longer periods (multiple bursts), and also analyze the potential benefits on localization introducing stronger requirements on the signal parameters, in particular the symbol width and the rise-time.

REFERENCES

- [1] Cospas-Sarsat Council, "Cospas-Sarsat 406 MHz MEOSAR Implementation Plan," Tech. Rep. R.012, Revision 8, Cospas-Sarsat, 2012.
- [2] K. Wang, Z. Dong, and S. Wu, "Research on FOA and TOA Estimation Algorithm of Galileo SAR Signal," in *Int. Conference on Inform. Eng. and Comput. Sci.*, Dec. 2010, pp. 1–5.
- [3] V. B. Nicolau, M. Coulon, Y. Grégoire, T. Calmettes, and J-Y Tournet, "Modified Cramer-Rao lower bounds for TOA and symbol width estimation. An application to search and rescue signals," in *Proc. IEEE Int. Conf. Acoust., Speech, Signal Process. (ICASSP)*, Vancouver, 2013.
- [4] A. N. D'Andrea, U. Mengali, and R. Reggiannini, "The modified Cramér-Rao bound and its application to synchronization problems," *IEEE Trans. Commun.*, vol. 42, no. 234, pp. 1391–1399, Feb. 1994.
- [5] E. D. Kaplan and C. J. Hegarty, *Understanding GPS: principles and applications*, Artech House, 2006.
- [6] Cospas-Sarsat Council, "Specification for Cospas-Sarsat 406 MHz distress beacons," Tech. Rep. T.001, Revision 13, Cospas-Sarsat, 2012.
- [7] S. M. Kay, *Fundamentals of Statistical Signal Processing: Estimation theory*, Prentice Hall, 1993.
- [8] J. G. Proakis and M. Salehi, *Digital Communications*, Mc-Graw Hill, Boston, 5th edition, 2008.
- [9] D. Rife and R.R. Boorstyn, "Single tone parameter estimation from discrete-time observations," *IEEE Trans. Inf. Theory*, vol. 20, no. 5, pp. 591–598, Sept. 1974.
- [10] S. Houcke, A. Chevreuil, and P. Loubaton, "Blind equalization - Case of an Unknown Symbol Period," *IEEE Trans. Signal Process.*, vol. 51, no. 3, pp. 781–793, March 2003.
- [11] P. Closas, C. Fernandez-Prades, and J.A. Fernandez-Rubio, "Cramér-Rao Bound Analysis of Positioning Approaches in GNSS Receivers," *IEEE Trans. Signal Process.*, vol. 57, no. 10, pp. 3775–3786, 2009.